ELSEVIER

Materials Science and Engineering A358 (2003) 266–272

MATERIALS SCIENCE & ENGINEERING A

www.elsevier.com/locate/msea

Microstructure and mechanical properties of tantalum after equal channel angular extrusion (ECAE)

Q. Wei [a,*], T. Jiao [a], S.N. Mathaudhu [b], E. Ma [c], K.T. Hartwig [b], K.T. Ramesh [a]

[a] *Department of Mechanical Engineering, Johns Hopkins University, Latrobe 200, Baltimore, MD 21218, USA*
[b] *Department of Mechanical Engineering, Texas A&M University, College Station, TX 77843-3123, USA*
[c] *Department of Materials Science and Engineering, Johns Hopkins University, Baltimore, MD 21218, USA*

Received 20 February 2003; received in revised form 3 April 2003

Abstract

We have investigated the microstructure and mechanical properties of equal channel angular extruded (ECAE) Ta. Mechanical properties were measured both under quasi-static loading and dynamic loading (in the latter case, the compression Kolsky bar technique was employed to attain strain rates of $\sim 10^3$ s^{-1}). It is shown that four passes of ECAE with route C at room temperature, which results in an equivalent strain of ~ 4.64, increases the strength of Ta by a factor of 2–3 under quasi-static loading, and by a factor of more than 1.5 under dynamic loading. Under quasi-static loading, the ECAE processed samples exhibit almost elastic-perfect plastic behavior; under dynamic loading, slight softening is observed, presumably due to adiabatic heating. It is found that ECAE decreases the strain rate sensitivity. Comparison of the X-ray diffraction (XRD) between the un-processed and ECAE processed Ta indicates significant broadening of the XRD peaks in the ECAE processed sample. Transmission electron microscopy reveals textured, elongated substructures with an average size of about 200 nm, and the substructures are separated by small angle grain boundaries. This work shows the potential for the production of ultra-fine grained or even nano-structured refractory metals with high melting points by using severe plastic deformation. Signs indicating increased shear localization tendancy were observed at high strain rates.

Keywords: Severe plastic deformation; ECAE; Microstructure; Mechanical properties; Refractory metals; Tantalum

1. Introduction

The past two decades have witnessed remarkable advances in processing and characterization of materials with ultra-fine grains (UFG) in the submicrometer and nanometer range. There are several processing routes for the production of such nano-structured materials (NSMs) [1]. Among these processes, the inert gas condensation technique pioneered by Gleiter [2] only produces NSMs in powder form. Subsequent compaction and densification to full density has been a great challenge. The major stumbling block is grain growth during consolidation of the nanometer-sized powder, diminishing the unique characteristics of the nanostructure. Another problem associated with powder metallurgy for NSMs is the introduction of impurities during the course of processing. So far, contamination, imperfect particle bonding and volume flaws such as porosity have been the major artifacts that adversely influence the properties of nano-structured metals. They are also the origin of controversies in the interpretation of various experimental observations of the mechanical properties [3]. As pointed out by Koch and Narayan [3] the use of a 'two-step' (powder production and consolidation) process to obtain bulk samples can be both expensive and problematic.

The equal channel angular extrusion (ECAE) technique invented and pioneered by Segal [4–7] is a technique that can produce truly bulk, fully dense and contamination-free metals with sub-micron to nanoscale grain sizes. Recently, this technique has seen a renaissance due to the rising interest in the microstructure and properties

* Corresponding author. Tel.: +1-410-516-5162; fax: +1-410-516-4316.
E-mail address: qwei@pegasus.me.jhu.edu (Q. Wei).

0921-5093/03/$ - see front matter
doi:10.1016/S0921-5093(03)00305-8

of NS or UFG materials. Briefly, the technique subjects a metal to severe plastic deformation through a simple shear process with little, if any change in the cross-sectional area of the work piece. It has been shown that the total strain accumulated through a series of repetitive pressings, ε_N, is

$$\varepsilon_N = N\frac{2}{\sqrt{3}}\cot\Phi \quad (1)$$

where N is the total number of passes through the die and Φ is the angle between the channels [4]. From this equation, it is seen that with a right angle ($\Phi = 90^\circ$) die, an equivalent strain of about 1.16 is achieved for a single pass. If the intersection between channels is not sharp, then non-uniform strains and lower strains result [4].

The ECAE process has been successfully used to produce a variety of metallic materials with UFG or NS microstructures. They include pure fcc metals such as Al, Cu, Ni, bcc metals such as Fe, hcp metals such as Ti, and alloys such as steels and Al alloys [8–16]. These materials, however, have relatively low melting temperatures. It would be of interest both scientifically and technically to investigate the evolution in microstructure and mechanical behavior during ECAE of refractory metals with relatively high melting temperatures. These metals include bcc Mo, Ta, and W. The present work reports microstructure and mechanical property results of Ta given four ECAE passes under both quasi-static and dynamic loading.

2. Experimental procedure

The original material is commercially pure (99.98%) tantalum that was vacuum arc remelted, and supplied by H.C. Starck Inc. The as-received bars have nominal dimensions of $25 \times 25 \times 150$ mm and contain large columnar grains with grain diameters larger than 5 mm. The original bars were processed using ECAE followed by a heat treatment at around 1065 °C in vacuo for 90 min to obtain grains in the range of 20–100 μm. This material was then used for further ECAE processing, which was performed in 90° tooling with a punch speed of 5.1 mm s^{-1} using route C for four passes (an equivalent strain of 4.64), at room temperature [17]. Route C processing returns material elements to their original shape after an even number of successive extrusions.

The material that was processed through route C for four passes has been tested for mechanical properties under quasi-static loading and dynamic loading. Specimens for mechanical testing were cut from the extruded billets using wire electrical discharge machining (EDM). Specimen dimensions for quasi-static loading are $1.7 \times 1.7 \times 2.6$ mm (rectangular shape); specimen dimensions for dynamic loading are $2.0 \times 2.0 \times 1.6$ mm. Quasi-static compressive loading with strain rates in the range of 10^{-3} to 10° s^{-1} was performed using an MTS hydro-servo system. Dynamic compressive loading with strain rates of around 10^3 s^{-1} was performed using the Kolsky bar (or split Hopkinson bar) technique where the specimen is sandwiched between two elastic bars (called the input and output bars). Strain gages are cemented on the elastic bars to measure (i) the incident pulse generated by an impacting projectile, (ii) the reflected pulse from the input bar/specimen interface and (iii) the transmitted pulse through the specimen to the output bar. Details of the Kolsky bar technique can be found in [18]. To observe the deformation behavior of the specimens under both quasi-static and dynamic compressive loadings, the side faces of the specimens were polished to a mirror finish. In the dynamic loading case, a DRS Hadland Ultra 8 high-speed camera with the ability to record 10^8 frames per second was employed to obtain a movie of the dynamic deformation of the specimens. The purpose was to clarify whether shear banding is involved in the plastic deformation of the tested material. For comparison, quasi-static and dynamic compressive tests were also performed on the un-processed Ta control samples.

The microstructure of the material that was ECAE processed through four passes using route C was investigated using transmission electron microscopy (TEM). The TEM specimens were EDM cut from the flow plane (billet side plane) of the processed billet, and thinned mechanically to a thickness of around 50 μm. Disks of 3 mm diameter were punched out of the thinned sheet, and were immersed in a petri dish of solution $50\%HF + 50\%HNO_3$ [19], followed by cleaning in ethanol, acetone and methanol before loading into the TEM. TEM observations were conducted using a Philip EM420 operated at 120 kV.

3. Results and discussion

Fig. 1 presents the true stress–strain curves obtained during quasi-static compressive loading of the ECAE Ta. The ECAE processed Ta behaves in a nearly elastic-perfectly plastic manner at these strain rates (i.e. little strain hardening is observed). Yield strengths above 700 MPa are recorded, with the strength increasing slightly with the strain rate at which the test was performed (a strength increase of 5% with a rate increase from 10^{-2} to 10° s^{-1}). For comparison, quasi-static compression tests were also conducted on the 'un-processed' Ta that was annealed at 1065 °C and the results are also displayed in Fig. 1. Now lower strengths are observed, as is a lower-yield-point, substantial strain hardening, and more rate sensitivity than evident in the as-processed material (note the strength increase of 50%

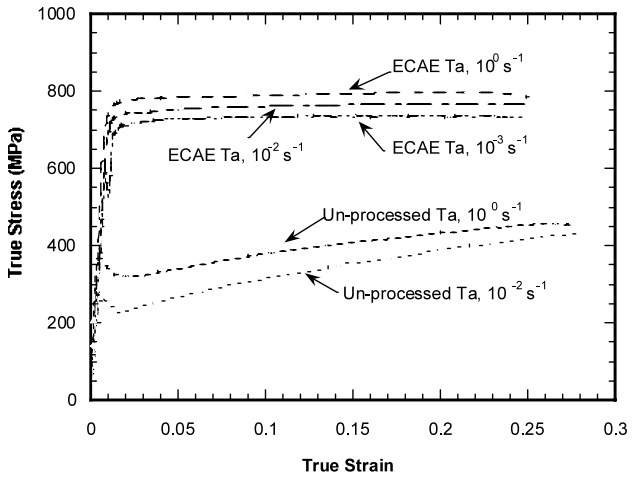

Fig. 1. Quasi-static compressive stress–strain curves for ECAE processed Ta as well as the un-processed Ta. The equivalent strain induced by the ECAE process is about 4.64.

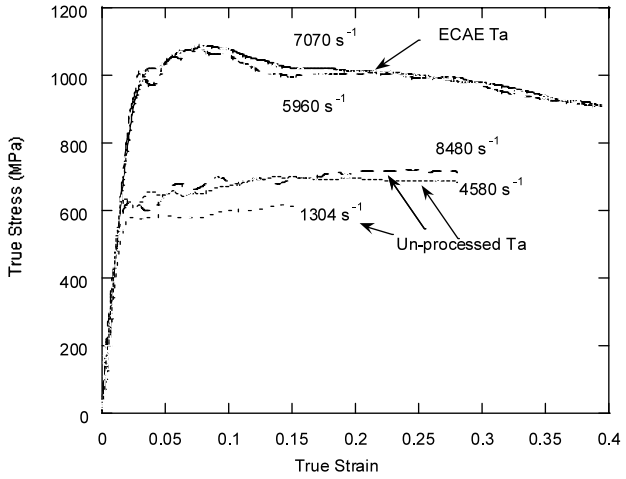

Fig. 2. Dynamic (compression Kolsky bar) stress–strain curves for ECAE processed Ta (equivalent strain induced by the ECAE process is ~4.64) as well as the un-processed Ta. Strain rates are noted in the figure.

with a rate increase from 10^{-2} to 10° s^{-1}). Comparing the results from the ECAE processed Ta and the un-processed Ta given in Fig. 1, we see that the ECAE enhances the yield strength of Ta by a factor of at least two, decreases the strain hardening, and decreases the rate dependence by an order of magnitude (note that grain size reduction in Fe from the micron scale to a few hundred nanometers also leads to a decrease in strain rate sensitivity [20]). The dependence of Vickers hardness on the grain size of the ECAE processed Ta has been reported to follow the Hall–Petch relation [17]:

$$\mathrm{VHN}_{300} = 78 + 69l^{-1/2} \tag{2}$$

where VHN_{300} is the Vickers hardness number under a load of 300 gf, and l is the average grain diameter. By using the approximate relationship between the Vickers hardness and the yield strength of a metal, we can estimate (using the strengths observed in Fig. 1) the sub-grain size of the ECAE processed Ta to be around 200 nm. The current TEM observations given below are consistent with this estimate.

Fig. 2 presents typical stress–strain curves for the ECAE processed Ta deformed at high strain rates. A yield stress of about 1.0 GPa is observed under dynamic compression. Instead of strain hardening, an apparent strain softening can be observed as a result of adiabatic heating under these high strain rates. The adiabatic temperature rise ΔT, developed in such an experiment is

$$\Delta T = \frac{\beta}{pC_{\mathrm{p}}} \int_0^{\varepsilon_{\mathrm{f}}} \sigma \, \mathrm{d}\varepsilon, \tag{3}$$

where β is the fraction of plastic work converted into heat (assumed to be 0.9 in this case), ρ is the density, C_{p} is the specific heat, σ is the flow stress and ε_{f} is the final strain. The corresponding temperature rise would be about 200 K when the strain is about 0.4. Significant temperature sensitivity of the stress–strain response is typical of bcc metals [21–23], including Ta, resulting in the apparent softening observed here. This is exacerbated by the fact that severe plastic deformation in the ECAE processed Ta almost exhausts the strain hardening capacity of the material by the introduction of a heavily deformed microstructure with high densities of dislocations and small grain sizes. For comparison, high-strain-rate test results on the un-processed Ta are also presented in Fig. 2; these results are consistent with those obtained by Perez-Prado et al. [21] on annealed Ta with a similar microstructure. Comparison of the quasi-static and dynamic stress–strain curves of the un-processed samples indicates that the strain hardening in the un-processed Ta under dynamic loading has decreased, again as a result of the near-adiabatic heating that can occur in such high-rate experiments. Note that

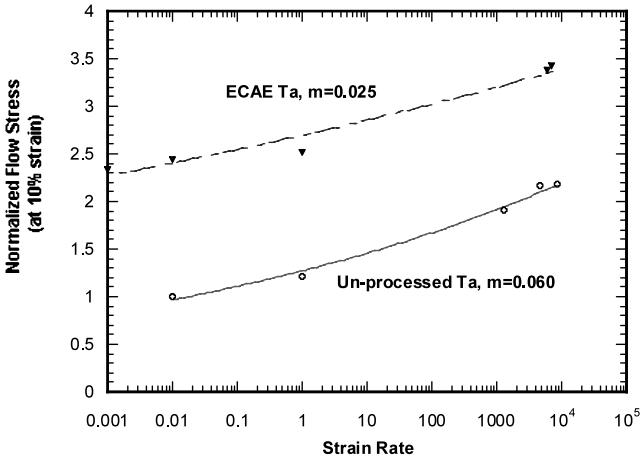

Fig. 3. Strain rate dependence of the un-processed Ta and the ECAE processed Ta. Power law curve fitting was used to obtain the strain rate sensitivity m.

the lower strengths of the un-processed Ta result in smaller temperature rises during any given experiment than would be observed in the ECAE Ta. Fig. 3 displays the rate dependence of the ECAE processed Ta along with the un-processed Ta. The flow stresses of all the samples at an off-set strain of 0.10 were normalized against the flow stress at 10% strain of the un-processed Ta under a strain rate of 10^{-2} s^{-1}. A power law in the form of $\sigma/\sigma_0 = (\dot{\varepsilon}/\dot{\varepsilon}_0)^m$ was used to fit the data, and the value of m is used as an indicator of the rate dependence of the material. It is seen, again, that the ECAE processed Ta exhibits decreased rate sensitivity as compared to the un-processed Ta (note, however, that some of the apparent reduction in rate-sensitivity is due to the additional thermal softening that occurs in the ECAE Ta).

Shear banding was observed to be the predominant plastic deformation mode for another bcc metal (Fe) with UFG or NS microstructure processed by mechanical attrition followed by consolidation [24,25]. Here, high-speed camera movies and post-loading surface structures analysis indicate localized shear deformation in the ECAE processed Ta only at the high loading rates. Fig. 4 shows three high-speed camera images taken at different time of dynamic loading, corresponding to zero strain, a strain of 8.1% and a strain of 18.6%, respectively. Some non-uniform deformations are developed at the largest strains post-mortem optical microscopy of the test samples showed that uniform plastic deformation also occurred.

Fig. 5 is an optical micrograph of the un-processed Ta, showing an average grain size of $\sim$20 μm. Fig. 6 is the X-ray diffraction (XRD) pattern of this annealed Ta, showing sharp peaks corresponding to the reflections for bcc Ta; the XRD result of the ECAE processed Ta given also in Fig. 6 exhibits significant broadening of all the peaks. This broadening arises mainly from the refining of the coherently diffracting domains, and it can be used to roughly estimate the sub-grain size of the specimen on the basis of the Warren–Averbach equation [26] or the modified Warren–Averbach equation for severely worked metals [27].

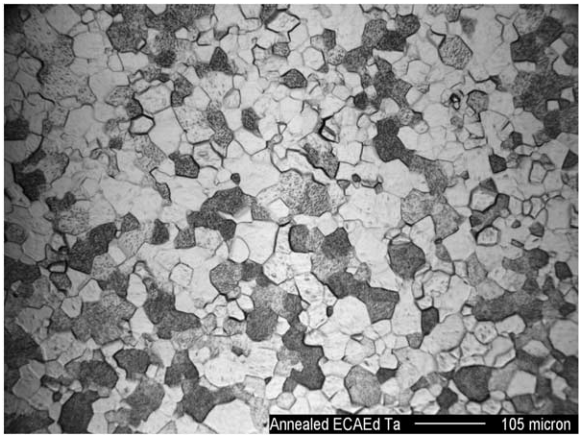

Fig. 5. Optical micrograph of the un-processed Ta, showing a relatively uniform equi-axed grain structure, with a grain size of approximately $\sim$20 μm.

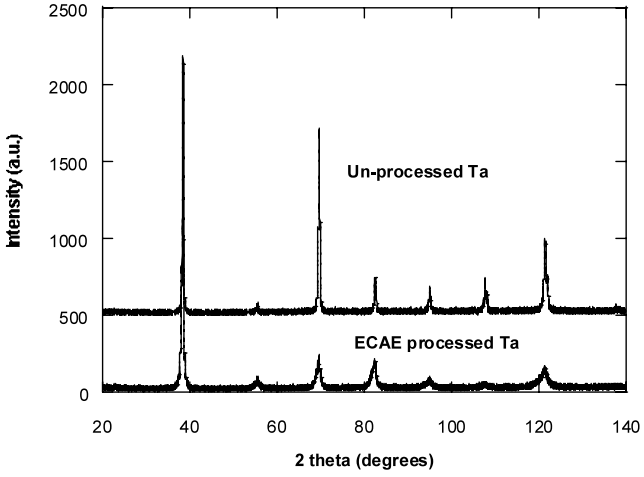

Fig. 6. XRD of un-processed and ECAE processed Ta. The former shows sharp reflections from bcc Ta, while the latter shows significant broadening of all the peaks.

TEM was performed to obtain detailed information about the microstructure of the ECAE processed Ta. Generally, the previously large grains ($\sim$20 μm, see Fig. 5) have been refined significantly. Sub-grains or substructures with varied sizes have been observed, ranging from a few hundred nanometers to below 100 nm. Fig. 7

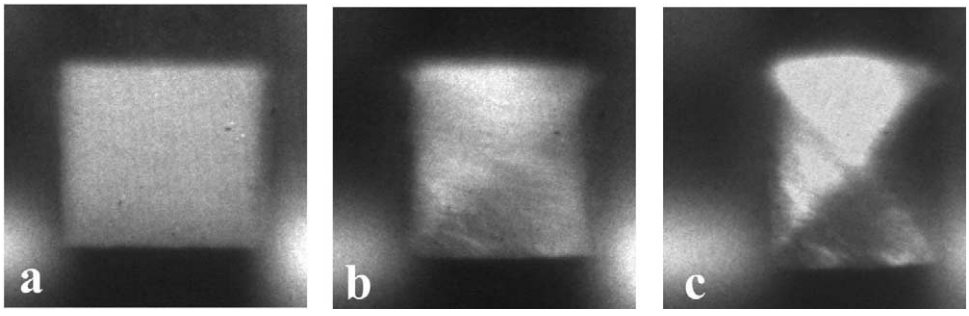

Fig. 4. High-speed camera images of the ECAE processed Ta during dynamic compressive loading at different deformation stages: (a) before loading; (b) 19 μs after commencement of loading (corresponding to a strain of 0.08); (c) 36 μs after commencement of loading (corresponding to a strain of 0.186). Note the localized deformations along the diagonal directions.

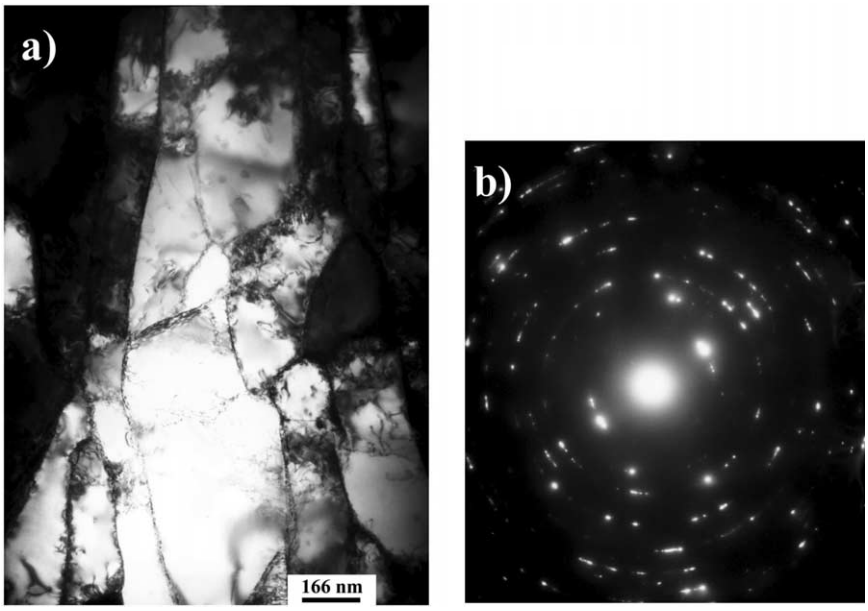

Fig. 7. Bright-field flow plane TEM micrograph (a) of the ECAE processed Ta (route C for four passes, with equivalent strain of $\sim$4.64), showing both elongated and equi-axed substructures and the accompanying SAD pattern (b) showing apparent concentration on the {1 1 0} reflections, indicating low angle boundaries between the substructures.

shows a bright-field TEM image of Ta that has experienced four passes of ECAE, with an equivalent strain of about 4.64. Here, a more or less elongated substructure with a width of $\sim$200 nm is observed, with smaller sub-grains inside the elongated grains. The diffraction spots in the selected area diffraction (SAD) pattern given in Fig. 7(b) demonstrate that the sub-structures are separated by low angle grain boundaries. Fig. 8(a) is the bright-field TEM image from another area of the same sample, again showing elongated grains of much smaller size. The SAD pattern given in Fig. 8(b) again indicates the low angle nature of the boundaries between the sub-grains. The interior of the substructures (cells) is clean and almost dislocation free. We have also observed considerable break-ups in the elongated sub-structures, with even finer substructure size than that in Figs. 7 and 8, again separated by small angle grain boundaries. In some cases, what looks like an original grain boundary is still visible, which encircles the much finer sub-grains.

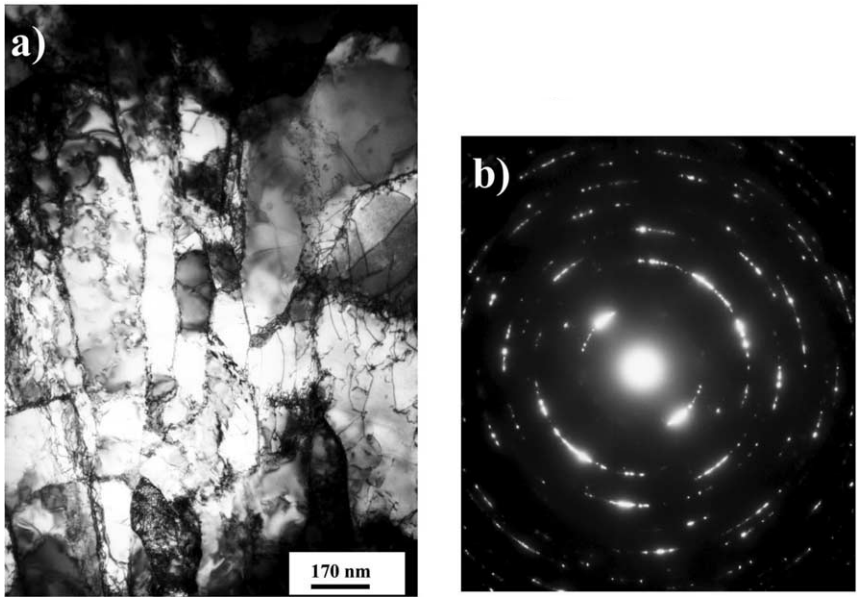

Fig. 8. Bright-field flow plane TEM micrograph (a) of the ECAE processed Ta (route C for four passes, with equivalent strain of $\sim$4.64), showing both elongated substructures with break-ups inside; the accompanying SAD pattern (b) showing apparent concentration on the {1 1 0} reflections, indicating low angle boundaries between the substructures.

As pointed out in Section 2, the ECAE route that was used to process Ta in this work was route C. The various routes of ECAE are defined as follows [28]. In route A the sample is not rotated between consecutive extrusion; route B_A denotes 90° rotations in alternate directions between each extrusion; route B_C denotes 90° rotation in the same direction between each extrusion and route C denotes a rotation of 180° between each extrusion. Extensive studies have been conducted on the effect of various factors of the ECAE process on the microstructure of the worked material, such as number of passes, temperature, extrusion speed, the size of the work piece, different routes, etc. [29–37]. It has been reported that route B_C is effective for producing an equiaxed sub-grain structure with high angle grain boundaries. Other routes, including route C that is used in this work, tend to produce elongated sub-grain structures with low angle grain boundaries [38–40].

There is a paucity of documented work in the processing and characterization of UFG refractory metals, such as Mo, Ta and W. The present work, together with those on ECAE processed W [41,42], show that severe plastic deformation may be a promising technique for the production of refractory metals with UFG structures. It should be pointed out that the work on W reported in [41,42] was conducted at 1000 °C. The results on Ta presented above confirm that microstructural refinement is significant, and there is room for improvement, including the use of more ECAE passes and/or different ECAE routes, and the effect of temperature. Note that a strength increase by a factor of 2–3 in the case of quasi-static loading, and a factor of more than 1.5 in the case of dynamic loading, have been achieved through only four passes.

4. Summary and concluding remarks

(1) Four ECAE passes with route C at room temperature increase the quasi-static strength of Ta by a factor of at least 2, and increase the dynamic strength by a factor of about 1.5.

(2) The ECAE processed Ta shows elastic-perfectly plastic behavior under quasi-static loading, with no strain hardening. Slight softening is observed for the processed Ta under dynamic loading, presumably due to adiabatic heating.

(3) ECAE processing decreases the strain rate sensitivity of the material. Most specimens deform uniformly, but at the high loading rates signs of localized shear become visible (c).

(4) It was confirmed that ECAE is a promising technique for refining the microstructure of refractory metals into the UFG regime. Four passes of ECAE with route C refines the grain size from more than 20 μm of the original material to a microstructure consisting of substructures of around 100–200 nm as previously reported [17]. The substructures have an elongated geometry with break-ups inside. Most of the substructures are separated by small angle boundaries.

Acknowledgements

This work was performed under the auspices of the Center for Advanced Metallic and Ceramic Systems (CAMCS) at the Johns Hopkins University. This research was sponsored by the Army Research Laboratory (ARMAC-RTP) and was accomplished under the ARMAC-RTP Cooperative Agreement No. DAAD19-01-2-0003. The views and conclusions contained in this document are those of the authors and should not be interpreted as representing the official policies, either expressed or implied, of the Army Research Laboratory or the US Government. The US Government is authorized to reproduce and distribute reprints for Government purposes not withstanding any copyright notation hereon.

References

[1] C. Suryanarayan, Inter. Mater. Rev. 40 (1995) 41–63.
[2] H. Gleiter, Acta Mater. 48 (2000) 1.
[3] C.C. Koch, J. Narayan, MRS Symp. Proc. 634 (B5.1.3) 2001.
[4] V.M. Segal, Mater. Sci. Eng. A 197A (1995) 157.
[5] V.M. Segal, K.T. Hartwig, R.E. Goforth, Mater. Sci. Eng. A 224A (1997) 107.
[6] V.M. Segal, Mater. Sci. Eng. A 271A (1999) 322–333.
[7] R.Z. Valiev, A.V. Korznikov, R.R. Mulyukov, Mat. Sci. Eng. A 168 (1993) 141–148.
[8] T.C. Lowe, R.Z. Valiev (Eds.), Investigations and Applications of Severe Plastic Deformation, Kluwer Academic Publishers, 2000.
[9] Y.T. Zhu, T.G. Langdon, R.S. Mishra, S.L. Semiatin, M.J. Saran, T.C. Lowe (Eds.), 'Ultrafine Grained Materials II', Annual Meeting and Exhibition, TMS, 2002.
[10] K. Neishi, Z. Horita, T.G. Langdon, Mater. Sci. Eng. A 325 (2002) 54.
[11] D.H. Shin, B.C. Kim, Y.S. Kim, K.T. Park, Acta Mater. 48 (2000) 2247.
[12] D. Jia, Y.M. Wang, K.T. Ramesh, E. Ma, Y.T. Zhu, R.Z. Valiev, Appl. Phys. Lett. 79 (2001) 611.
[13] K.T. Park, Y.S. Kim, J.G. Lee, D.H. Shin, Mater. Sci. Eng. A 293 (2000) 165.
[14] J. Kim, I. Kim, D.H. Shin, Scripta Mater. 45 (2001) 421.
[15] D.H. Shin, B.C. Kim, K.T. Park, W.Y. Choo, Acta Mater. 48 (2000) 3245.
[16] R.Z. Valiev, R.K. Islamgaliev, I.V. Alexandrov, Prog. Mater. Sci. 45 (2000) 103.
[17] K.T. Hartwig, S.N. Mathaudhu, H.J. Maier, I. Karaman, in: Y.T. Zhu, T.G. Langdon, R.S. Mishra, S.L. Semiatin, M.J. Saran, T.C. Lowe (Eds.), Ultrafine Grained Materials II, TMS, 2002.
[18] P.S. Follansbee, The Hopkinson bar, in: J.R. Davis, S.K. Refnes (Eds.), Metals Handbook, vol. 8, ninth ed., ASM, Metals Park, Ohio, 1985, pp. 198–203.
[19] G. Thomas, M.J. Goringe, Transmission Electron Microscopy of Materials, Wiley, 1979.
[20] D. Jia, Ph.D. Thesis, The Johns Hopkins University, 2001.

[21] M.T. Perez-Prado, J.A. Hines, K.S. Vecchio, Acta Mater. 49 (2001) 2905.
[22] T. Suzuki, Y. Kamimura, H.O.K. Kirchner, Philos. Mag. A 79 (1999) 1629.
[23] J.W. Christian, Metall. Trans. 14A (1983) 1237.
[24] Q. Wei, D. Jia, K.T. Ramesh, E. Ma, Appl. Phys. Lett. 81 (2002) 1240.
[25] D. Jia, K.T. Ramesh, E. Ma, Scripta Mater. 42 (2000) 73.
[26] B.E. Warren, X-Ray Diffraction, Dover Publications Inc, 1990.
[27] T. Ungar, in: T.C. Low, R.Z. Valiev (Eds.), Investigations and Applications of Severe Plastic Deformation, Kluwer Academic Publishers, 2000, pp. 93–102.
[28] M. Furukawa, Z. Horita, M. Nemoto, T.G. Langdon, J. Mater. Sci. 36 (2001) 2835.
[29] K. Nakashima, Z. Horita, M. Nemoto, T.G. Langdon, Acta Mater. 46 (1998) 1589.
[30] P.B. Berbon, M. Furukawa, Z. Horita, M. Nemoto, T.G. Langdon, Metall. Mater. Trans. 30A (1999) 1989.
[31] M. Furukawa, Y. Iwahashi, Z. Horita, M. Nemoto, T.G. Langdon, Mater. Sci. Eng. 257A (1998) 328.
[32] A. Yamashita, D. Yamaguchi, Z. Horita, T.G. Langdon, Mater. Sci. Eng. 284A (2000) 100.
[33] Z. Horita, T. Fujinami, T.G. Langdon, Mater. Sci. Eng. 318A (2001) 34.
[34] M. Furukawa, Z. Horita, M. Nemoto, R.Z. Valiev, T.G. Langdon, Philos. Mag. 78A (1998) 203.
[35] C. Xu, T.G. Langdon, Scripta Mater. 48 (2003) 1.
[36] D. Yamaguchi, Z. Horita, M. Nemoto, T.G. Langdon, Scripta Mater. 41 (1999) 791.
[37] S.L. Semiatin, P.B. Berbon, T.G. Langdon, Scripta Mater. 44 (2001) 135.
[38] T.G. Langdon, M. Furukawa, Z. Horita, M. Nemoto, in: T.C. Lowe, R.Z. Valiev (Eds.), Investigations and Applications of Severe Plastic Deformation, Kluwer Academic Publishers, 2000, p. 149.
[39] Y. Iwahashi, Z. Horita, M. Nemoto, T.G. Langdon, Acta Mater. 46 (1998) 3317.
[40] K. Oh-ishi, Z. Horita, M. Furukawa, M. Nemoto, T.G. Langdon, Metall. Mater. Trans. 29A (1998) 2011.
[41] I.V. Aleksandrov, G.I. Arab, L.O. Shostakovich, A.R. Kil'mametov, R.Z. Valiev, Phys. Met. Metall. 93 (2002) 493.
[42] I.V. Aleksandrov, G.I. Raab, V.U. Kazyhanov, L.O. Shestakova, R.Z. Valiev, R.T. Dowding, in: Y.T. Zhu, et al. (Eds.), Ultrafine Grained Materials II, TMS, 2002, pp. 199–207.